Tuning ferroic states in La doped $BiFeO_3$-$PbTiO_3$ displacive multiferroic compounds

L. F. Cótica,[1,2,a)] V. F. Freitas,[2] O. A. Protzek,[2] J. A. Eiras,[3] D. Garcia,[3] F. Yokaichiya,[4] I. A. Santos,[4] R. Guo,[1] and A. S. Bhalla[1]
[1]*Department of Electrical and Computer Engineering, University of Texas at San Antonio, One UTSA Circle, San Antonio, Texas 78249, USA*
[2]*Department of Physics, State University of Maringá, Maringá, PR 87020-900, Brazil*
[3]*Department of Physics, Federal University of São Carlos, São Carlos, SP 13565-905, Brazil*
[4]*Nuclear and Energy Research Institute, São Paulo, SP 05508-000, Brazil*

(Received 27 March 2014; accepted 5 July 2014; published online 17 July 2014)

In this manuscript, X-ray and high-resolution neutron powder diffraction investigations, associated with Rietveld refinements, magnetic hysteresis curves and a modeling of electron-density distributions around the ions, are used to describe the driving forces responsible for tuning the ferroic states in La doped (0.6)$BiFeO_3$-(0.4)$PbTiO_3$ compositions. The intrinsic relations between the ferroic orders and the structural arrangements (angles, distances and electron-density distributions around the ions) are revealed, helping in the understanding of some aspects comprising the ferroic properties of perovskite-based displacive multiferroic compounds. © *2014 AIP Publishing LLC*.
[http://dx.doi.org/10.1063/1.4890455]

I. INTRODUCTION

Multiferroic magnetoelectric materials, which show simultaneous ferroelectric and magnetic orders, have been the subject of broad range studies due to their potential for advanced technological multifunctional applications, such as non-volatile multiple state memories and magnetically tunable piezodevices.[1] The origin of magnetic and ferroelectric orders has also been intensively investigated in order to know and control, separately and/or simultaneously, the multiferroic characteristics, aiming to use multiferroics in macroscopic devices.[2] However, the microscopic physical mechanisms which control such properties have not been conclusively established yet. In this context, the La doped (0.6)$BiFeO_3$–(0.4)$PbTiO_3$ (BFPT-yL, where y is the La concentration) compositions emerge as optimal alternatives to study and elucidate the mechanisms that control the ferroelectric, magnetic, and structural properties in displacive multiferroics because (1-x)$BiFeO_3$–(x)$PbTiO_3$ (BFPTx) solid solutions are known to present simultaneous ferroelectricity, piezoelectricity, and magnetic orders (anti or weak-ferromagnetism) at room temperature.[3] From the structural point of view BFPTx compositions show the coexistence of rhombohedral (*R*3*c* space group) and tetragonal (*P*4*mm*) phases at $x \sim 0.3$ forming a morphotropic phase boundary (MPB) region where the polarization response is intensified.[4] Interestingly, BFPT-yL compositions also show a MPB region for $y \sim 3$, where rhombohedral (*R*3*c*) and tetragonal (*P*4*mm*) phases also coexist, and the polarization response is also intensified while the magnetic state/response is preserved.[5] Recently,[6] a whole set of piezoelectric coefficients, as well as magnetic and ferroelectric parameters,[5] were reported for the BFPT-yL compositions confirming them as promising candidates for practical piezoelectric, ferroelectric, and magnetoelectric applications, whereas they show tunable ferroelectric/piezoelectric properties and magnetic orders at room temperature. It is also worth mentioning that La addition in tetragonal (0.6)$BiFeO_3$–(0.4)$PbTiO_3$ ceramics improves electrical resistivity and releases the unit cell tetragonality (*c*/*a* ratio), consequently, diminishing the ceramics brittleness.[5,7,8] In fact, increased electrical resistivities (from 10^{12} to 10^{13} Ω cm) and remnant magnetizations (from 0.06 to 0.14 emu/g) were reached in La doped BFPTx compositions.[3,9] Similarly, the d_{33} piezoelectric coefficient also increases (from 10 to 278 pC/N) with the increasing of the La concentration in BFPTx compositions, as reported by Leist *et al.*[10] Interestingly, La addition also decreases the ferroelectric Curie temperature and the dielectric constant.[3,9] Furthermore, ferroelectric responses (coercive field, remnant and saturation polarizations) are also very sensitive to the La addition.[3,8,9] However, it is worth mentioning that the modification of the perovskite A site with La does not promotes major changes in the BFPT magnetic ordering since Fe^{3+} magnetic ions are located in the perovskite B site, forming the magnetic network. In this context, the application of powder diffraction techniques, as X-ray (XPD) and neutron (NPD) powder diffraction, can shed some light on the intrinsic features beyond the multiferroism in BFPT-yL compositions.[11] Indeed, by the complete description of structure or structural alterations, magnetic states can also be indirectly investigated by diffraction techniques.[11,12]

In this work, a complete description of the coupling mechanism responsible for the magnetic response, as well as its intrinsic relations with the structure of BFPT-yL compositions (angles, distances between atoms and electron-density distributions around the ions), is presented considering the quantum mechanism responsible for the indirect magnetic superexchange interaction. Besides, by using XPD and high-

a)Author to whom correspondence should be addressed. Electronic mail: lfcotica@dfi.uem.br. Visiting faculty at University of Texas at San Antonio.

 © 2014 AIP Publishing LLC

Reuse of AIP Publishing content is subject to the terms at: https://publishing.aip.org/authors/rights-and-permissions. Download to IP: 200.130.19.195 On: Wed, 24 Aug 2016 14:28:17

resolution NPD (HR-NPD) data associated with Rietveld refinements, magnetic hysteresis curves, and modeling the electron-density distributions around the ions, a detailed description on the driving forces that control the magnetic, ferroelectric, and structural properties of BFPT-yL compositions is presented. This description helps in the understanding of some aspects comprising the improvement and control of the ferroic properties of perovskite-based displacive multiferroic compounds.

II. METHODS

Stoichiometric powders of BFPT-yL compositions, with $y = 0$, 3, 5, 10, 20, and 30 wt. %, were synthesized by using analytical graded (Aldrich) Bi_2O_3, Fe_2O_3, PbO, TiO_2, and La_2O_3 powders. Samples were optimally processed by high-energy ball milling as previously reported.[5,13] Room temperature XPD analyses were conducted with a Shimadzu XRD-7000 X-ray diffractometer (Cu k_α radiation). HR-NPD patterns were collected using the high-resolution diffractometer E9 at the BERII reactor at Hahn-Meitner-Institut (Helmholtz-Zentrum Berlin). The neutron diffraction measurements were conducted at room temperature with an incident neutron wavelength of 1.798 Å.

The HR-NPD data, carrying magnetic and structural information, were analyzed by applying the Rietveld method using the FullProf package.[14] The HR-NPD data were best described by a structural model consisting of a conventional structure ($P4mm$ and/or $R3c$ space groups) to describe nuclear scattering, and another purely magnetic structure (magnetic Fe^{3+} ions in a G-type antiferromagnetic (AFM) order) to describe the magnetic scattering. The magnetic structure was obtained by a reversal operator, **R**, combined with a standard crystal symmetry operation (-1 point group) and a triclinic symmetry ($P1$), in the so-called irreducible representation (IR), as previously reported.[12,15]

In order to confirm the crystal structures and obtain the electron density maps, the XPD data were refined by using the Rietveld method and the same crystallographic data as obtained via HR-NPD analyses in the Rietan-FP program.[16] After the structural refinements, by using the Rietan-FP output file, the electron density map's calculations were carried out. Regarding the methodology used in calculations, the maximum entropy method (MEM) is a powerful way to obtain electron density information. It is a well-established high-resolution technique commonly used for reconstructing precise electron density maps from X-ray diffraction data.[17,18] MEM is also more accurate for the reconstruction of electron densities than using inverse Fourier transforms, because it overcomes information losses (experimental noise) by maximizing the information entropy.[17] In fact, this method is based on Shannon's information theory[19] that considers the loss of information in compressing and transmitting data that have some noise by using the equation $S(X) = -k\Sigma p_i \ln(p_i)$, where $S(X)$ is the entropy of the random variable X and P is the entropy probability distribution. Following these ideas, MEM consists in find a probability distribution that maximizes the information entropy.[19] The application of MEM to crystallographic problems was proposed by Collins.[17] In the Collins formalism, an iterative procedure based on constrained entropy maximization is used to reconstruct the electron density maps by using X-ray diffraction data. In this work, we used the PRIMA code,[20] a program for calculation of electron densities from observed structure factors by means of the maximum entropy method. The visualization of structural arrangements and electron-density distributions around the ions was performed by using the three-dimensional structure viewer program VESTA (Visualization for Electronic and Structural Analysis–3.0.7).[16]

Room temperature magnetic characterizations were performed using a LakeShore (7307–7 Inch) vibrating sample magnetometer.

III. RESULTS AND DISCUSSIONS

Room temperature magnetization curves for BFPT-yL samples are shown in Fig. 1. A typical weak-ferromagnetic behavior can be seen in the magnetic curves of low La concentrated samples (Fig. 1—insets: from (i) to (iv)) as the overlap of antiferromagnetic (unsaturated magnetization curves) and slight ferromagnetic (small coercive field, H_c, and remnant magnetization, M_r, in the hysteresis curves) responses. However, in compositions with high La concentrations ($y = 20$ and 30), the hysteretic behavior is more pronounced (Figs. 1(e) and 1(f)), suggesting a well-defined weak-ferromagnetic character. This behavior indicates a change in the quantum interaction between magnetic ions (spin interactions) with La addition, as discussed below.

XPD and HR-NPD patterns obtained for the BFPT-30La composition are shown in Figs. 2(a) and 2(b), respectively. The insets (XPD, Fig. 2(a) and HR-NPD, (Fig. 2(b)) are representative diffraction patterns with better visualization (20°–60° 2θ range) for different La concentrations. Both diffraction patterns were refined by using the Rietveld method and the obtained structural, magnetic, and reliability factors are listed in Table I. As can be seen in insets of Fig. 2(a), the structural symmetry changes with the increasing of La concentration from a tetragonal ($P4mm$, for $y = 0$) to a rhombohedral ($R3c$, for $y = 5$) symmetry, passing through a MPB region ($y \sim 3$). Considering the HR-NPD results, the relevant magnetic information is highlighted by the pure magnetic scattering pattern, observed as a peak at $2\theta \sim 22.7°$ (Fig. 2(b)), along others that are superimposed with structural peaks. The magnetic scattering patterns were best fitted using a G-type AFM model, which is considered a magnetic pseudo-cubic structure with magnetic moments ferromagnetically ordered in the (111) plane, but antiferromagnetically ordered with the adjacent plane.[21]

These results show that the magnetic moment per ion reached higher values for the highest La concentration (4.96 μ_B, BFPT-30 L) as shown in Table I. Interestingly, samples with high La concentrations also show more intense macroscopic magnetic responses, i.e., higher H_c and M_r in the hysteresis curves (Figs. 1(e), 1(f), and Fig. 3(b)). Coincidentally, there is a decrease in lattice parameters and

Reuse of AIP Publishing content is subject to the terms at: https://publishing.aip.org/authors/rights-and-permissions. Download to IP: 200.130.19.195 On: Wed, 24 Aug 2016 14:28:17

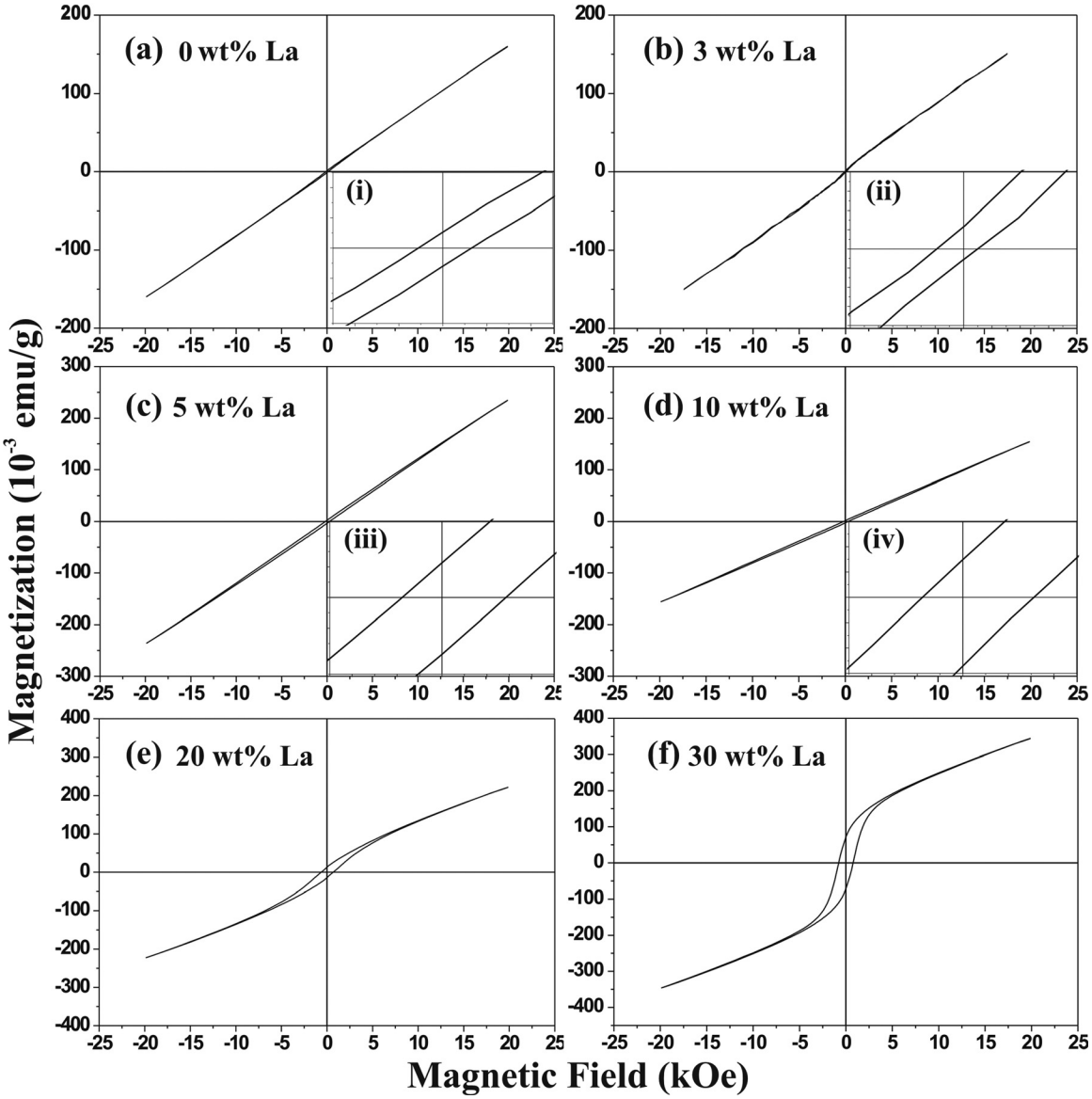


FIG. 1. Room temperature magnetic hysteresis curves for La doped (0.6)$BiFeO_3$-(0.4)$PbTiO_3$ samples. Insets (i)–(iv) enlarged visions of the low magnetic field regions.

unit cell volumes with the increase in La concentration. These findings indicate a strong link between magnetic properties and structural characteristics in BFPT-yL samples.

To investigate the structure/properties relations, the perovskite structural arrangements, i. e., the rhombohedral (*R*3*c* space group, yellow (online), or light gray lines), hexagonal (black lines), and magnetic pseudocubic (red (online) or dark gray dotted lines) unit cells used to describe the crystal structure of BFPT-yL samples are shown in Fig. 3(a). The superexchange interaction is shown schematically by the intertwined magnetic network (Fe^{3+} - O^{2-} - Fe^{3+}, red (online) or dark gray thicker lines), which interconnects all Fe^{3+} ions and promotes the antiferromagnetic order in $BiFeO_3$-based systems. However, in (1-x)$BiFeO_3$–(x)$PbTiO_3$ samples (x = 0.4 in this case), the completely compensated antiferromagnetic coupling is broken by the substitution of Fe^{3+} ions in the B perovskite site by Ti^{4+} ions, giving order to magnetic clusters. Furthermore, the superexchange interaction is very sensitive to the geometric/spatial arrangement ($\theta_{S\text{-}Ex}$ angle and distance ($d_{S\text{-}Ex}$) between Fe^{3+} ions, Fig. 3(a)). Interestingly, M_r, $d_{S\text{-}Ex}$, and $\theta_{S\text{-}Ex}$ parameters, obtained from the M × H curves and from the Rietveld refinement of X-ray and HR-NPD data (shown in Fig. 3(b)) clearly reveal that since $\theta_{S\text{-}Ex}$ increases with the increase in La concentration (tend to 180°), the remnant magnetization is also increased, while the $d_{S\text{-}Ex}$ (blue (online) or light gray dashed line) decreases. These results suggest an increasing in the interaction between some magnetic ions due to the decreasing in the distance ($d_{S\text{-}Ex}$) between the magnetic sublattices, i. e., the nature of the quantum magnetic interaction can be changed in this process. In fact, as Fe^{3+} ions become closer to each other, a more direct exchange interaction can start to take place, resulting in a more weak-ferromagnetic-like induced ordering, as addressed in Figs. 1(e) and 1(f).

It is worth noting that the substitution Bi^{3+}/Pb^{2+} ions by La^{3+} ones in the A perovskite site promotes all the identified

Reuse of AIP Publishing content is subject to the terms at: https://publishing.aip.org/authors/rights-and-permissions. Download to IP: 200.130.19.195 On: Wed, 24 Aug 2016 14:28:17

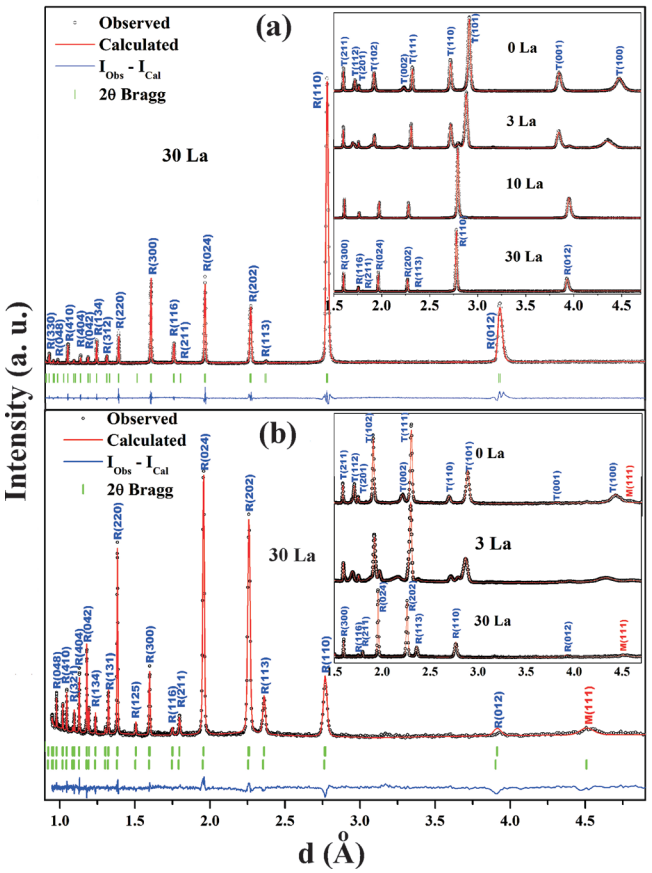


FIG. 2. Rietveld refinement of (a) X-ray and (b) high-resolution neutron powder diffraction patterns of La doped (0.6)$BiFeO_3$-(0.4)$PbTiO_3$ compositions. Insets: enlarged relevant regions for different La concentrations.

changes in magnetic properties and structural arrangements of BFPT-yL compositions. In this way, an intriguing issue remains: can (and how) these alterations act on the ferroelectric order of the BFPT-yL compositions? Indeed, it is well known that for $y = 0$, coercivity and remnant field are prevented in ferroelectric hysteresis loops due to the high tetragonality,[5,6] while for $y = 3$ or 5, or other BFPT compositions in the MPB region, coercivity and remnant field are extremely enhanced.[5,7,11] Furthermore, for high La concentrations ($y = 10$, 20, or 30), the hysteretic response is prevented due to electrical conductivity.[5] In this way, and for understanding this complex scenario, electron-density distributions around the ions were modeled (Fig. 4, (100) plane, for example) by using the structural refinement results and the VESTA program. As a result, from the electron density plots, it is possible to address an increase in La^{3+} ions concentration (until $y = 5$) which causes a decrease in the electron localization around A_2-O bonds (hybridization between Bi,Pb(6s,6p) and O(2p) orbitals),[22] indicating a continuous weakening of this bond. Beyond this La^{3+} concentration ($y > 5$), a large distortion occurs in the structure and the Bi,Pb(6s,6p) and O(2p) orbitals' overlap is increased around the A_4-O bonds, strengthening this bond. This behavior leads to great impacts in the ferroic properties of these materials because the structural distortions tend to directly promote major changes in the ferroelectric properties, also indirectly promoting changes in magnetic ones. The main change occurs in the B-O_1 and B-O_4 bonds (hybridization between Fe,Ti(3d) and O(2p) orbitals—Fig. 4, (200) plane),[22] where the electron-density distributions related to Fe,Ti(3d)/O(2p) orbitals overlapping are strongly enhanced for $y = 20$ and 30. In this way, the magnetic properties are directly affected by this increased overlapping, leading to an increasing on $\theta_{S\text{-}Ex}$ and a decreasing on the distance between magnetic ions ($d_{S\text{-}Ex}$) and, consequently, starting the direct interaction between Fe^{3+} ions (direct exchange interaction resulting in the ferromagnetic order (Figs. 1(e) and 1(f)).

TABLE I. Rietveld refinement results of neutrons and X-ray diffraction data for La doped (0.6)$BiFeO_3$-(0.4)$PbTiO_3$ compositions. Lattice parameters and volume for tetragonal (a_T, c_T, and V_T) and rhombohedral (a_R, c_R, and V_R) phases, atomic positions for the main (higher concentration) symmetry ($Z_{Bi/Pb/La}$, $Z_{Fe/Ti}$, X_O, Y_O, Z_O, and Z_{O2}-2nd tetragonal site), magnetic moment by atom (μ_{Fe}/μ_B), and reliability factors (Rp, Rwp, and χ^2).

Parameter	X-ray diffraction						Neutron Powder diffraction		
Space group	*P4mm*	*P4mm* + *R3c*		*R3c*			*P4mm*	*P4mm* + *R3c*	*R3c*
La (wt. %)	0	3	5	10	20	30	0	3	30
a_T (Å)	3.8385(2)	3.8502(5)	3.8587(6)	—	—	—	3.8321(7)	3.8553(5)	—
c_T (Å)	4.4573(9)	4.3538(8)	4.3368(9)	—	—	—	4.4468(4)	4.3338(9)	—
V_T (%)	100	95.58	25.31	0	0	0	100	85.53	0
a_R (Å)	—	5.6006(0)	5.5971(5)	5.5899(3)	5.5743(2)	5.5578(4)	—	5.5925(1)	5.5633(8)
c_R (°)	—	13.7247(1)	13.7344(2)	13.6766(6)	13.6687(6)	13.6323(8)	—	13.6923(4)	13.5880(4)
V_R (%)	0	4.42	74.69	100	100	100	0	14.47	100
$Z_{Bi/Pb/La}$	−0.00169	−0.05040	−0.02988	−0.02952	−0.02630	−0.01897	−0.01198	−0.06718	0.05357
$Z_{Fe/Ti}$	0.56106	0.50123	0.20782	0.22211	0.21636	0.23080	0.54003	0.45609	0.30748
X_O	0.50000	0.50000	0.50277	0.45200	0.49151	0.49268	0.50000	0.50000	0.45195
Y_O	0.50000	0.50000	−0.50277	0.01700	0.04760	0.05026	0.50000	0.50000	−0.00884
Z_O	0.19036	0.10035	0.97615	0.95350	0.95568	0.96118	0.14631	0.07033	1.06222
Z_{O2}	0.65566	0.62129	—	—	—	—	0.66044	0.59172	—
μ_{Fe}/μ_B	—	—	—	—	—	—	3.82	3.74	4.96
R_p	16.9	16.8	26.6	16.7	21.6	15.3	17.8	20.8	21.3
R_{wp}	17.9	19.0	30.9	18.1	24.1	15.7	14.1	17.1	15.7
χ^2	5.48	8.31	8.89	9.63	1.70	4.23	1.99	2.49	1.75

Reuse of AIP Publishing content is subject to the terms at: https://publishing.aip.org/authors/rights-and-permissions. Download to IP: 200.130.19.195 On: Wed, 24 Aug 2016 14:28:17

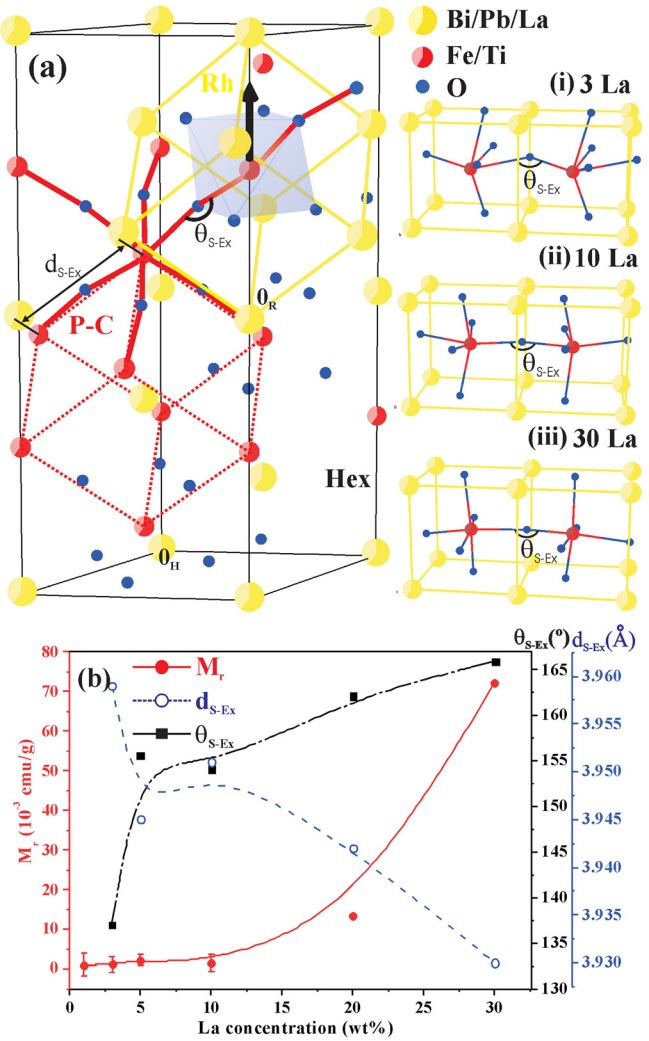


FIG. 3. Magnetic and structural features of BFPT-yL compositions. (a) Complete representation of structural symmetries: hexagonal (black line), rhombohedral (yellow (online) or light gray lines), and magnetic pseudocubic (red (online) or dark gray dot lines). Insets: Superexchange angles for (i) y = 3, (ii) y = 10, and (iii) y = 30 samples. (b) Magnetization, distance between Fe^{3+} ions (d_{S-Ex}) and superexchange angles (θ_{S-Ex}) as a function of La concentration.

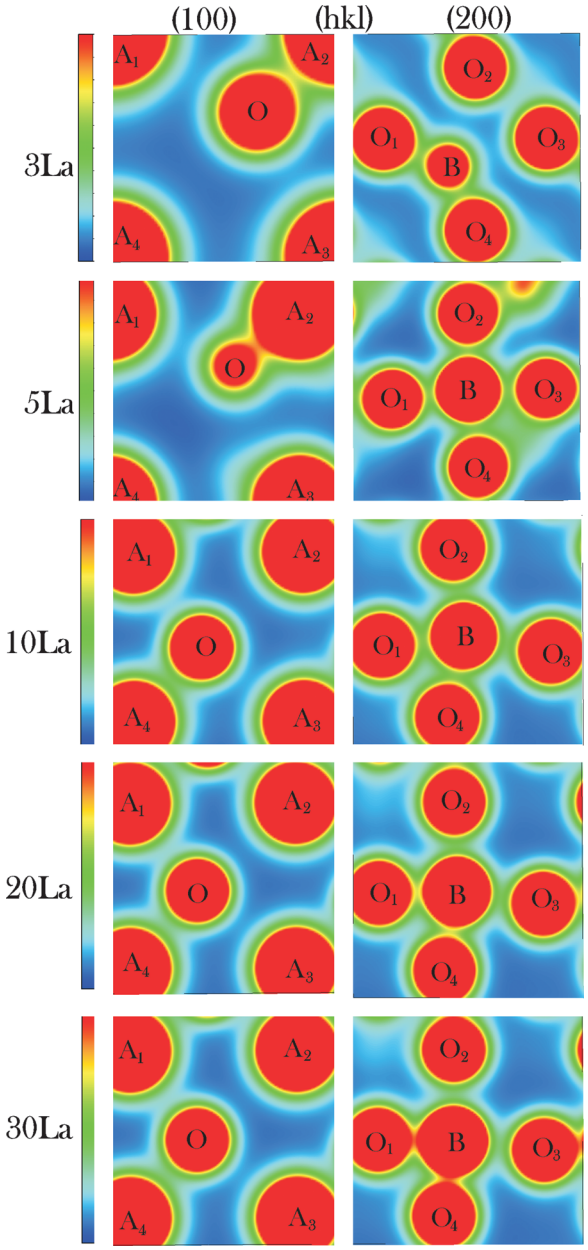


FIG. 4. Electron-density distributions in the perovskite ABO_3 type ($R3c$) for La doped (0.6)$BiFeO_3$-(0.4)$PbTiO_3$ compositions, showing the (100) and (200) planes. (Colors) red regions represent well-localized electrons in contrast with blue regions. Labels: A = Bi^{3+}/Pb^{2+}/La^{3+}, B = Fe^{3+}/Ti^{4+} and O = O^{2-}.

IV. SUMMARY

In summary, ferroelectric and magnetic properties of BFPT-yL compositions are affected by La addition and the consequent changes in the chemical bonds around ions. Interestingly, for BFPT-3L and BFPT-5L compositions, where the completely compensated antiferromagnetic coupling starts to be broken, the Bi,Pb(6s,2p)/O(2p) orbitals overlapping along the A_2-O bounds are intensified (Fig. 4 (100) plane), favoring the ferroelectric response, as recently reported by Fujii *et al.* for the $BiFeO_3$ compound.[23] On the other hand, weak-ferromagnetic order tends to takes place in high La concentrated BFPT-yL (y = 10, 20, and 30) compositions. In fact, La addition in the perovskite A site of BFPT compositions (probably in any other displacive and perovskite structured multiferroic magnetoelectric compounds) leads to decrease the active lone-pair concentration, releases the covalence character of the A_n-O bonds and, consequently, intensifies the B_n-O interactions. The most relevant aspect in this process is that all ferroic properties are completely tuned and controlled by La^{3+} addition (or any ion that preserve the structural stability and do not show active lone pairs) and also can be studied/accompanied by X-ray diffraction experiments.

ACKNOWLEDGMENTS

The authors would like to thank the Brazilian agencies CNPq (proc. 305129/2010-4), FAPESP (proc. 2008/04025-0), Fundação Araucária de Apoio ao Desenvolvimento Científico e Tecnológico do Paraná (Prots. 22825, 24202 and 22870), and CAPES (PROCAD 082/2007) for financial support. The neutron diffraction facilities, provided by the

Reuse of AIP Publishing content is subject to the terms at: https://publishing.aip.org/authors/rights-and-permissions. Download to IP: 200.130.19.195 On: Wed, 24 Aug 2016 14:28:17

Hahn-Meitner-Institut from the Helmholtz-Zentrum Berlin, are also gratefully acknowledged.

[1]W. Eerenstein, N. D. Mathur, and J. F. Scott, Nature **442**(7104), 759 (2006); N. A. Hill and A. Filippetti, J. Magn. Magn. Mater. **242**, 976 (2002).
[2]N. A. Spaldin, S. W. Cheong, and R. Ramesh, Phys. Today **63**(10), 38 (2010).
[3]J. R. Cheng and L. E. Cross, J. Appl. Phys. **94**(8), 5188 (2003).
[4]J. Chen, X. R. Xing, G. R. Liu, J. H. Li, and Y. T. Liu, Appl. Phys. Lett. **89**(10), 101914 (2006); S. A. Fedulov, P. B. Ladyzhinskii, I. L. Pyatigorskaya, and Y. N. Venevtsev, Sov. Phys. Solid State **6**(2), 375 (1964); W. M. Zhu, H. Y. Guo, and Z. G. Ye, Phys. Rev. B **78**(1), 014401 (2008).
[5]L. F. Cotica, F. R. Estrada, V. F. Freitas, G. S. Dias, I. A. Santos, J. A. Eiras, and D. Garcia, J. Appl. Phys. **111**(11), 114105 (2012).
[6]V. F. Freitas, I. A. Santos, E. Botero, B. M. Fraygola, D. Garcia, and J. A. Eiras, J. Am. Ceram. Soc. **94**(3), 754 (2011).
[7]H. Amorin, C. Correas, P. Ramos, T. Hungria, A. Castro, and M. Alguero, Appl. Phys. Lett. **101**(17), 172908 (2012).
[8]T. Leist, W. Jo, T. Comyn, A. Bell, and J. Rodel, Jpn. J. Appl. Phys. Part 1 **48**(12), 120205 (2009).
[9]J. R. Cheng, S. W. Yu, J. G. Chen, Z. Y. Meng, and L. E. Cross, Appl. Phys. Lett. **89**(12), 122911 (2006).
[10]T. Leist, T. Granzow, W. Jo, and J. Rodel, J. Appl. Phys. **108**(1), 014103 (2010).
[11]T. P. Comyn, T. Stevenson, M. Al-Jawad, W. G. Marshall, R. I. Smith, J. Herrero-Albillos, R. Cywinski, and A. J. Bell, J. Appl. Phys. **113**(18), 183910 (2013).
[12]V. F. Freitas, D. Z. Montanher, T. G. M. Bonadio, V. L. Mazzocchi, J. Mestnik, C. B. R. Parente, D. Garcia, J. A. Eiras, L. F. Cotica, and I. A. Santos, J. Appl. Phys. **114**(13), 134102 (2013).
[13]I. A. Santos, H. L. C. Grande, V. F. Freitas, S. N. de Medeiros, A. Paesano, L. F. Cotica, and E. Radovanovic, J. Non-Cryst. Solids **352**(32–35), 3721 (2006); V. F. Freitas, H. L. C. Grande, S. N. de Medeiros, I. A. Santos, L. F. Cotica, and A. A. Coelho, J. Alloys Compd. **461**(1–2), 48 (2008).
[14]J. Rodriguez-Carvajal, Appl. Crystallogr. 30 (2001).
[15]E. H. Kisi and C. J. Howard, *Applications of Neutron Powder Diffraction* (Oxford University Press, Oxford, 2008).
[16]F. Izumi and K. Momma, Solid State Phenom. **130**, 15 (2007).
[17]D. M. Collins, Nature **298**(5869), 49 (1982).
[18]T. Itoh, S. Shirasaki, Y. Fujie, N. Kitamura, Y. Idemoto, K. Osaka, H. Ofuchi, S. Hirayama, T. Honma, and I. Hirosawa, J. Alloys Compd. **491**(1–2), 527 (2010).
[19]P. Coppens, *X-Ray Charge Densities and Chemical Bonding* (Oxford University Press, New York, 1997).
[20]M. Yashima, N. Sirikanda, and T. Ishihara, J. Am. Chem. Soc. **132**(7), 2385 (2010).
[21]E. F. Bertaut, in *Magnetism III*, edited by G. T. Rado and H. Suhl (Academic Press, New York, 1963), p. 149.
[22]L. F. Cotica, V. F. Freitas, I. B. Catellani, I. A. Santos, D. Garcia, and J. A. Eiras, Appl. Phys. Lett. **101**(17), 172903 (2012); M. Yashima, K. Omoto, J. Chen, H. Kato, and X. R. Xing, Chem. Mater. **23**(13), 3135 (2011).
[23]K. Fujii, H. Kato, K. Omoto, M. Yashima, J. Chen, and X. R. Xing, Phys. Chem. Chem. Phys. **15**(18), 6779 (2013).

Reuse of AIP Publishing content is subject to the terms at: https://publishing.aip.org/authors/rights-and-permissions. Download to IP: 200.130.19.195 On: Wed, 24 Aug 2016 14:28:17